# Quantification of immobilization-induced changes in human calf muscle using speed-of-sound ultrasound

## An observational pilot study

Lisa Ruby, MD[a,*], Sergio J. Sanabria, PhD[a,b], Katharina Martini, MD[a], Thomas Frauenfelder, MD[a], Gerrolt Nico Jukema, MD[b,c], Orcun Goksel, PhD[d], Marga B. Rominger, MD[a]

## Abstract

Short-term immobilization leads to fatty muscular degeneration, which is associated with various negative health effects. Based on literature showing very high correlations between MRI Dixon fat fraction and Speed-of-Sound (SoS), we hypothesized that we can detect short-term-immobilization-induced differences in SoS.

Both calves of 10 patients with a calf cast on one side for a mean duration of $41 \pm 26$ days were examined in relaxed position using a standard ultrasound machine. Calf perimeters were measured for both sides. A flat Plexiglas-reflector, placed vertically on the opposite side of the probe with the calf in-between, was used as a timing reference for SoS. SoS was both manually annotated by two readers and assessed by an automatic annotation algorithm. The thickness values of the subcutaneous fat and muscle layers were manually read from the B-mode images. Differences between the cast and non-cast calves were calculated with a paired $t$ test. Correlation analysis of SoS and calf perimeter was performed using Pearson's correlation coefficient.

Paired $t$ test showed significant differences between the cast and non-cast side for both SoS ($P < .01$) and leg perimeter ($P < .001$). SoS was reduced with the number of days after cast installment ($r = -0.553$, $P = .097$). No significant differences were found for muscle layer thickness, subcutaneous fat layer thickness, mean fat echo intensity, or mean muscle echo intensity.

Short-term-immobilization led to a significant reduction in SoS in the cast calf compared to the healthy calf, indicating a potential role of SoS as a biomarker in detecting immobilization-induced fatty muscular degeneration not visible on B-mode ultrasound.

**Abbreviations:** CT = computed tomography, MRI = magnetic resonance imaging, SoS = speed of sound, US = ultrasound.

**Keywords:** Adipose tissue, immobilization, muscle atrophy, rehabilitation, speed of sound, ultrasonography

*[a] Zurich Ultrasound Research and Translation (ZURT), Institute of Diagnostic and Interventional Radiology, University Hospital Zurich, Zürich, Switzerland, [b] Deusto Institute of Technology, University of Deusto / IKERBASQUE, Basque Foundation for Science, Bilbao, Spain, [c] Department of Trauma, University Hospital Zurich, [d] Computer-assisted Applications in Medicine (CAiM), ETH Zurich, Zürich, Switzerland.*

*[*] Correspondence: Lisa Ruby, Zurich Ultrasound Research and Translation (ZURT), Institute of Diagnostic and Interventional Radiology, University Hospital Zurich, Rämistrasse 100, 8091 Zürich, Switzerland (e-mail: lisa.ruby@usz.ch).*

## 1. Introduction

Muscle atrophy occurs in the sequel of an injury or illness due to required immobilization or unloading.[1–3] During this episode, a rapid decline in muscle mass is observed. This is of great clinical importance as it is associated with various negative health effects, such as impaired muscle strength and reduced functional capacity as well as effects on the metabolism,[4,5] such as reduction of metabolic rate,[6] increased insulin resistance and increased body mass fat.[7,8]

The extent of muscle loss correlates with the length of hospital stay and the necessity of rehabilitation.[9] For the elderly population, a reduction in muscle mass leads to a decreased energy absorption during falls.[10] It has been suggested that short periods of muscle disuse lead to the origin of age-related fatty muscular degeneration.[11] Studies indicate that not only the loss of muscle but also the accumulation of intermuscular adipose tissue, which is known for its endocrine features, contribute to the clinical sarcopenia symptoms.[12] Immediate rehabilitation to restore muscle mass and function is of great importance.[13] Therefore, there is a need for a modality to identify patients who suffered substantial muscle loss in order to identify patients who suffered substantial muscle loss.

State-of-the-art imaging techniques to assess muscle composition include dual x-ray absorptiometry, computed tomography (CT), magnetic resonance imaging (MRI), as well as ultrasound (US).[14] US offers several advantages, as it is inexpensive, broadly available and without exposure to ionizing radiation.

Ultrasound elastography aims at quantifying mechanical properties of tissue. However, muscoluskeletal shear-wave elastography is highly susceptible to confounders, such as changes of probe/muscle fiber angle and muscle activation states.[15–17]

Speed of sound (SoS) is a quantitative imaging biomarker, which measures the speed of propagation of longitudinal waves in tissues and is dependent on the material, through which it travels.[18] The difference between the nominal SoS value of fat (1440 m/s) and muscle (1585 m/s) is about 10%.[18] Intermediate SoS values correspond to a mixture of these two extremes. Measuring SoS therefore allows for quantification of adipose tissue fat fraction, as shown by several studies for liver[19] and muscle.[20] For musculoskeletal ultrasound, *Ruby et al found very strong correlations between SoS and the total fat fraction of the same lower leg muscle volume section assessed with the reference standard Dixon MRI.[19]

Immobilization-induced changes in muscle SoS have not been investigated to the best of our knowledge. SoS could potentially be a portable method for the quantification of fat in muscle,[21] which could facilitate early detection of muscle loss and enable appropriate measures.

Based on literature stating that short-term immobilization leads to fatty muscular degeneration,[22] we hypothesized that we can detect immobilization-induced differences in SoS, serving as a potential biomarker of fatty degeneration in muscle.

## 2. Materials and methods

### 2.1. Study design

This prospective, single-institution study was approved by the institutional review board and local ethics committee. Patients were chosen from the traumatology clinic as they were clinically scheduled for a cast renewal or removal in the timeframe April to June 2018. Inclusion criterion was the installation of a calf cast on one side with coverage of the lower leg from the base of the toes until ~2 cm below the popliteal cavity (Fig. 1A). In order to minimize possible confounding of early post-traumatic changes, such as hemorrhage or edema, only patients with a minimum cast duration of 7 days were included. Foot casts or partial lower leg casts were not included in the study to ensure immobilization of the entire lower leg. Patients who were immobilized in a wheelchair or sustained a fracture, operation, sweeling or pain in the non-cast leg were excluded to avoid masking of an immobilization-induced difference between both legs (false negative).

### 2.2. Study participants

Using the data of the hospital information system, medical data including age, diagnosis, injury side, date of cast implementation, operations and weight bearing limit was aquired. A questionnaire, which involved parameters such as weight, height, activity level (0 = no activity, 1 = low activity [<200 m daily walking distance], 2 = higher activity [≥200 m daily walking distance]) was completed by the study participants.

### 2.3. Examination

Both calf muscles of 10 patients (median age 46 years, range 19–68) (Fig. 2) with a calf cast for a mean duration of $41 \pm 26$ days were examined with a standard ultrasound machine by one sonographer (L.R.). A plexiglas reflector was used as a timing reference for SoS (m/s, probe segment average) and placed on the opposite site of the hand-held 9-MHz linear probe with the superficial posterior compartment of the calf longitudinally in-between (Fig. 1B). The center of the reflector, which was labeled with an arrow for orientation purposes, was placed at the height of maximal calf perimeter. Both hand-held 9-MHz probe and reflector were kept in longitudinal direction with regard to the muscle fibers at the height of the greatest calf diameter, ~1 to 2 cm posterior to the tibial bone. The probe-reflector distance was defined to a tolerance of 0.1 mm with a positioning frame, which allowed controlling the distance between the probe and the reflector (calf thickness). The distance adjustment unit was positioned caudal of the probe and the reflector. Although measurements are principally possible in arbitrary positions, all study participants sat on a chair during the entire examination with a 90° flexion of the knee. The legs were in a relaxed state without any loading. We measured both calves in a fixed order, starting with the injured calf. Nine calves were examined twice by the same examiner by repeating the positioning protocol. Ultrasound lotion (PolySonic, Parker Laboratories, Inc, Fairfield, USA) was applied on the reflector and probe surfaces. The calf thickness was adjusted to achieve contact between the US probe, muscle and reflector. The calf thickness values were read from a digital distance sensor for SoS quantification with 0.01 mm digital resolution. In addition, the calf perimeter was assessed using a measuring tape.

## 3. Post-processing

### 3.1. SoS

A custom add-on software and an interface developed for this purpose were used for raw US data acquisition and SoS reading. For each element of the probe, an US pulse was transmitted and the same element recorded the received US echoes. Given a reflector echo time $t$ (in seconds) and the reflector-probe distance $d$, the SoS (in meters/second) is calculated as $SoS = 2*d/t$. A SoS segment is calculated at a defined measurement position by converting the time coordinate in the RF lines to SoS units according to $d$. The two readers (L.R., S.J.S.) manually marked the average SoS over the ultrasound probe width (Fig. 1C). In addition, an automatic algorithm was used to automatically read SoS values from the ultrasound images.[23]

### 3.2. B-mode post-processing

The thickness values of the subcutaneous fat and muscle layers were manually read from the B-mode images by the examiner (L.R.) Fat and muscle layers were segmented and the respective average echo intensity and standard deviation (SD) values were calculated.

## 4. Investigation of measurement reproducibility and confounders in volunteers

To assess the reproducibility of measurements, 10 repeated measurements of the left and right calves of a male and female volunteer were performed with the probe and reflector placed in the same positions as for the patients. Reflector and probe were removed and replaced for each measurement. Keeping the probe-reflector distance values and the height position within the muscle constant, sequential measurements were performed with
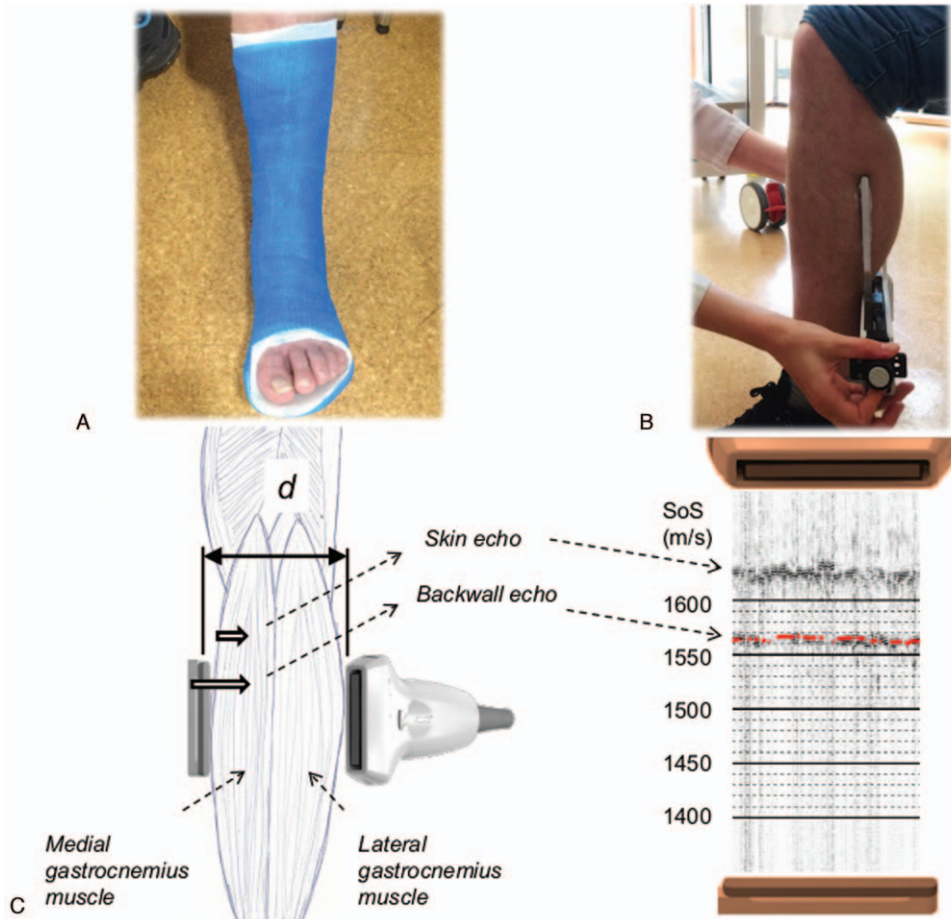
**Figure 1.** Examination set-up. (A) Patient with a cast, (B) A plexiglas reflector was used as a timing reference for SoS (m/s, probe segment average). Reflector and hand-held 9-MHz linear probe were located in the sagittal plane 1 to 2 cm posterior to the tibial bone with the calf longitudinally in between. The center of the reflector was placed at the height of maximal calf perimeter. (C) The skin and reflector back wall echoes can be identified. The plexiglas plate, which we used as reflector, has a thickness of 5 mm and two reflecting surfaces. One reflecting surface is in direct contact with the skin (skin echo). The other reflecting surface is the back wall of the reflector, that is, the reflection after the ultrasound wave propagates 5 mm within the reflector, bounces back, propagates another 5 mm and is again coupled through the skin. SoS values of the back wall echo, which is less contaminated by artifacts and thus more attractive for speed-of-sound measurements, were annotated manually and by an automated algorithm (line marked in red).
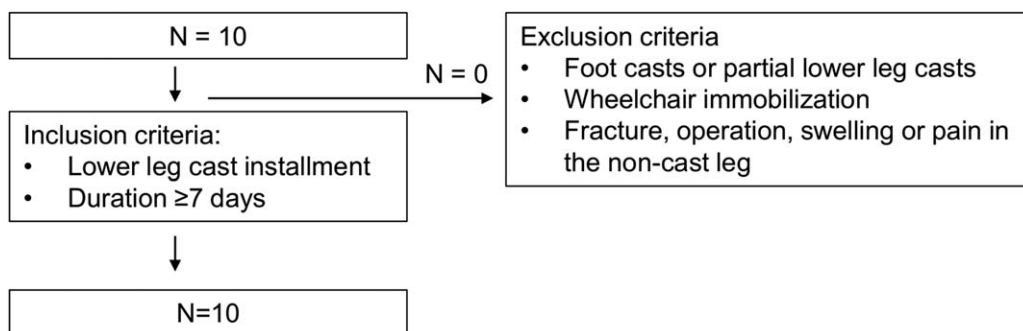


**Figure 2.** Flowchart. Patients with a lower leg cast for a duration of at least 7 days were included in the study. Patients who were immobilized in a wheelchair or sustained a fracture, operation, swelling, or pain in the non-cast leg were excluded.
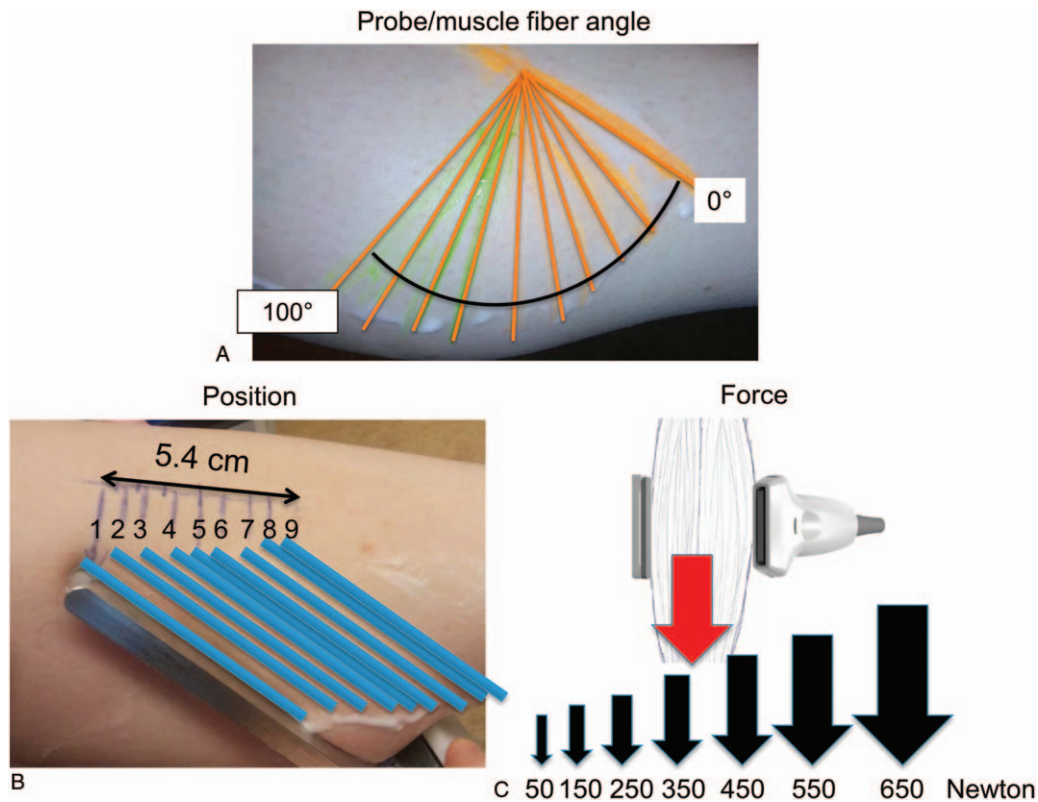
**Figure 3.** Confounder setup. Analysis of confounding factors in SoS measurements: The effect of varying probe/muscle fiber orientation angle (A), parallel displacements within the muscle (B) and varying force (C), displacements within the muscle (B) and varying force (C) were assessed.

the probe-reflector angle changing in equal steps with regard to the muscle fibers from 0° (parallel to the fiber) to 100° (Fig. 3A). To investigate the influence of the position within the muscle, probe and reflector were parallely displaced over a distance of 5.4 cm (Fig. 3B) and nine measurements were performed, while the probe-fiber orientation and probe-reflector distance were kept constant. To assess the effect of muscle load on SoS measurements, SoS was measured at different activation states, which were controlled with a body weight scale (accuracy ± 1 kg), while the distance, position index and probe-fiber angle were kept unchanged. The calf was loaded isometrically at a controlled stable force level (ranging from 5 to 65 kg (in 10 kg steps), corresponding to 50 to 650 N) and the ultrasound probe was re-positioned at the maximum calf diameter position in parallel orientation to the muscle fibers (Fig. 3C).

### 4.1. Statistical analysis

In order to detect small SoS differences induced by immobilization that might be masked by the baseline SoS variations among patients, we used paired statistical analysis based on the differences between the two calves for SoS, layer thicknesses, echo intensities and calf perimeter. Pearson's correlation coefficient was used to assess correlations of SoS differences between both calves with patient characteristics, days since cast installment and perimeter differences. Intraclass correlation coefficient (ICC) and Bland-Altman were calculated to assess intra-examiner and inter-reader agreement. For the investigation of reproducibility and confounders of measurements, standard deviation (SD) values were assessed.

## 5. Results

Patient characteristics and measured calf perimeter values are listed in Table 1. For SoS, we found a Pearson's correlation coefficient of $-0.207$ ($P=.565$) with BMI and $0.179$ ($P=.620$) with age.

**Table 1**

**Patient anthropometric and injury-related information.**

| Parameter | Value |
| --- | --- |
| Perimeter healthy calf (mean ± SD) | 37.4 ± 3.6 |
| Perimeter cast calf (mean ± SD) | 34.4 ± 3.6 |
| Age (median, range) | 34.5 (19.0–68.0) |
| BMI (median, range) | 23.0 (17.9–33.8) |
| Injury side (in %) | ● Left (70%) |
| | ● Right (30) |
| Duration since cast instalment (mean ± SD) | 41.2 ± 26.2 |
| General activity during cast instalment (in %) | ● None (0) |
| | ● <200 m (10) |
| | ● ≥200 m (90) |
| Weight-bearing on cast calf (in %) | ● None (10) |
| | ● Partial (90) |
| | ● Full (0) |
| Injury (in %) | ● Talocrural joint fracture (70) |
| | ● Metatarsal fracture (10) |
| | ● Calcaneal fracture (10) |
| | ● Chronic wound of the plantar foot (10) |
| Injury required operation (in %) | ● YES (50) |
| | ● NO (50) |
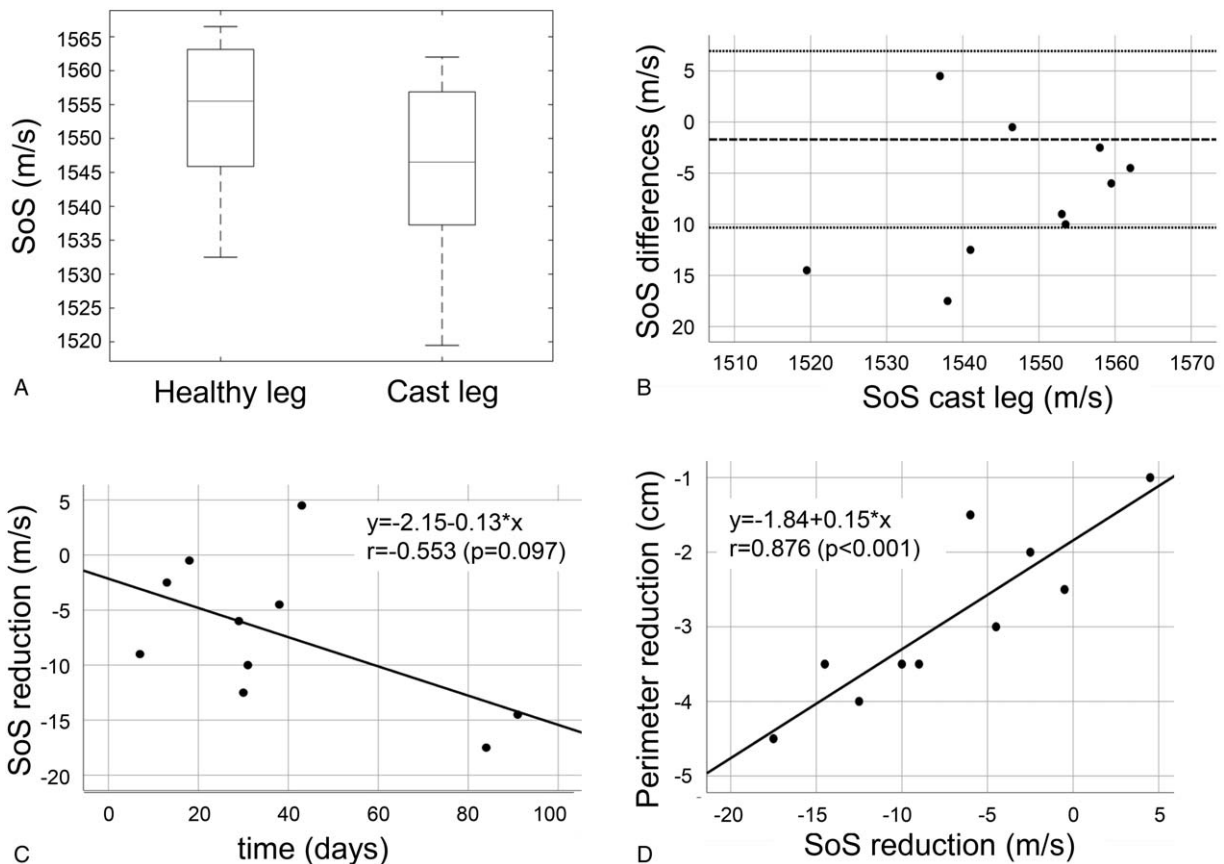
**Figure 4.** SoS and calf perimeter differences. (A) Boxplots indicating the SoS median and range in the healthy and cast calves. (B) Bland-Altman plot with the differences between both legs on the *y*-axis and the SoS values of the cast legs on the *x*-axis. (C) Line scatter plot displaying the mean days since cast installment (*x*-axis) and the SoS reduction in the cast calf compared to the non-cast calf (*y*-axis). (D) Line scatter plot showing the mean reduction in SoS (*x*-axis) and calf perimeter (*y*-axis).

### 5.1. Speed-of-Sound (SoS)

For 10 patients with a cast duration of at least 7 days, significantly lower values were found for calf perimeter ($P < .001$) and SoS ($P < .01$) (Fig. 4A and B) in the cast calves. Days after cast installment correlated with the SoS reduction in the cast calf compared to the healthy calf (Pearson $r = -0.553$, $P = .097$) (Fig. 4C). We found a Pearson correlation coefficient of 0.876 ($P < <0.001$) between the SoS reduction and perimeter reduction between the cast and healthy calf, respectively (Fig. 4D).

### 5.2. B-mode evaluation

Comparing the cast and healthy calves in the B-mode images, no significant differences were found regarding subcutaneous fat layer thicknesses (paired *t* test $P = .991$), muscle layer thickness (paired *t* test $P = .058$), mean echo intensity values of fat ($P = .801$) or mean echo intensity values of muscle ($P = .666$).

### 5.3. Intra-examiner

For 18 calves (9 patients), which were measured twice by the same examiner, we found an ICC of 0.850. The mean difference between the means of both measurements was 1.6 m/s with SoS differences ($\pm 1.96$ SD) ranging from $-14.5$ to 17.6 m/s (Fig. 5A). There was no significant correlation between probe-reflector

distance and SoS values ($r = 0.285$, $P = .223$). The probe-reflector distance among patients was in a range from 47.89 to 94.14 mm (repeated measurements out).

### 5.4. Inter-reader

We detected an ICC of 0.979 ($P < .001$) (average measures) between reader 1, reader 2 and the automatic annotation algorithm. The mean difference between the means of both manual readers and the automatic annotation was 0.53 m/s with SoS differences ($\pm 1.96$ SD) ranging from $-6.44$ to 7.51 m/s. Differences between the automatic annotation and the mean of both manual readers are illustrated by a Bland-Altman plot in Figure 5B.

### 5.5. Reproducibility of measurements and confounders

For the male volunteer, we found a mean of 1566.3 m/s with a SD of 4.5 m/s in the right and a mean of 1571.3 m/s with a SD of 4.8 m/s in the left calf (Fig. 6). For the female volunteer, the mean of 10 repeated measurements was 1560 m/s with a SD of 4.0 m/s in the right and 1563.5 m/s with a SD of 4.6 m/s in the left calf. Measuring SoS with different probe-muscle fiber angles in a range of 100°, the repeatability was given by SD = 1.75 m/s (Fig. 7A). For different locations within the muscle (Position index), we obtained a SD = 2.46 m/s (Fig. 7B). For differing muscle loading
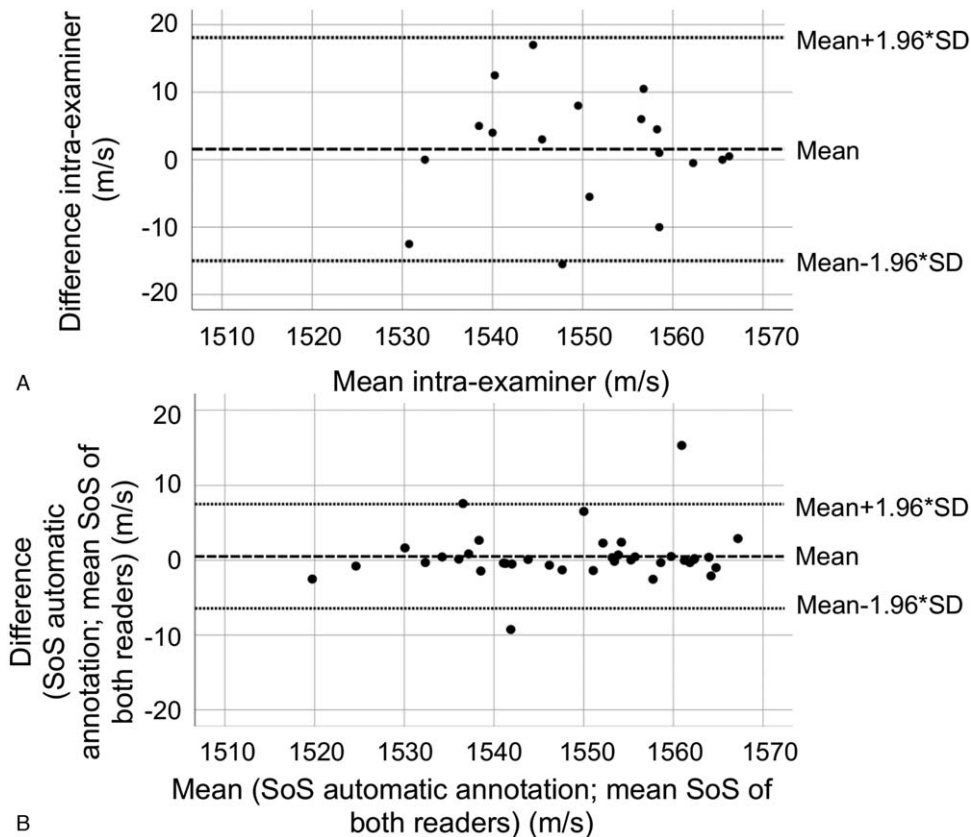
**Figure 5.** Intra-examiner and inter-reader (A) Intra-examiner for 9 repeated measurements of both legs. (B) Comparison of automatic annotation and means of both human readers (inter-reader).

states (Force), ranging from 50 to 650 N, we found a SD of 4.45 m/s (Fig. 7C).

## 6. Discussion

We found a significant reduction in SoS in the cast calf compared to the healthy calf, which was more pronounced with longer cast



**Figure 6.** Speed of Sound (SoS) measurement reproducibility. Boxplots showing ten repeated measurements of the left and right calves of a male and female volunteer to assess the reproducibility of measurements.

duration. In the B-mode image, no significant differences between both calves were detected for subcutaneous fat and muscle layer thicknesses or mean echo intensity values of fat and muscle. The effects of fiber orientation, muscle activation or positioning height were small and measurements showed a high reproducibility.

MRI is considered the reference standard for assessing fatty muscular degeneration.[14,24] Based on known SoS differences between muscular (1585 m/s) and adipose (1440 m/s) tissue,[18] strong correlations between SoS and the Dixon MRI fat fraction of the same volume section have been found for the lower leg.[20]

Several studies have shown that muscle inactivity increases inter- and intramuscular adipose tissue.[12,22,25–29] Similarly, significant differences between the healthy and immobilized leg could be explained by increased short-term immobilization-induced fatty degeneration. Another contributing factor to the detected difference in SoS between both calves could lie in the increased strain in the healthy calf, leading to an overall decrease in adipose and an increase in muscular tissue. Other studies, which have shown immobilization-induced reductions in muscle weight, muscle thickness and cross sectional area, are in line with our hypotheses.[29–35]

Welch et al found significantly larger muscle thicknesses in elderly living in extended care compared to those living independently,[36] whereas the comparison of the fat layers was not significant. We did not find a significant difference for fat or muscle mean echo intensity or thickness values between the healthy and cast calves. Therefore, SoS might have the potential to detect differences, which are not visible in B-mode images.
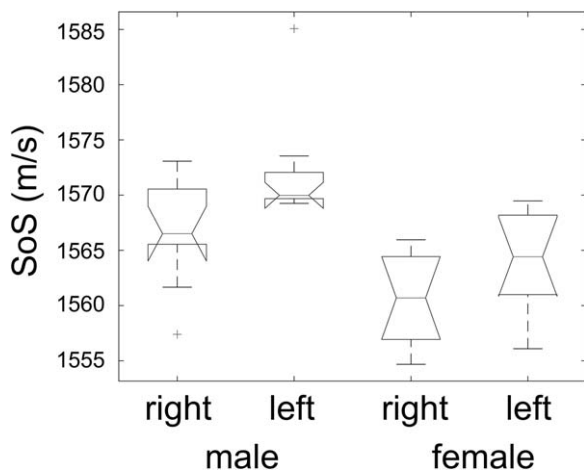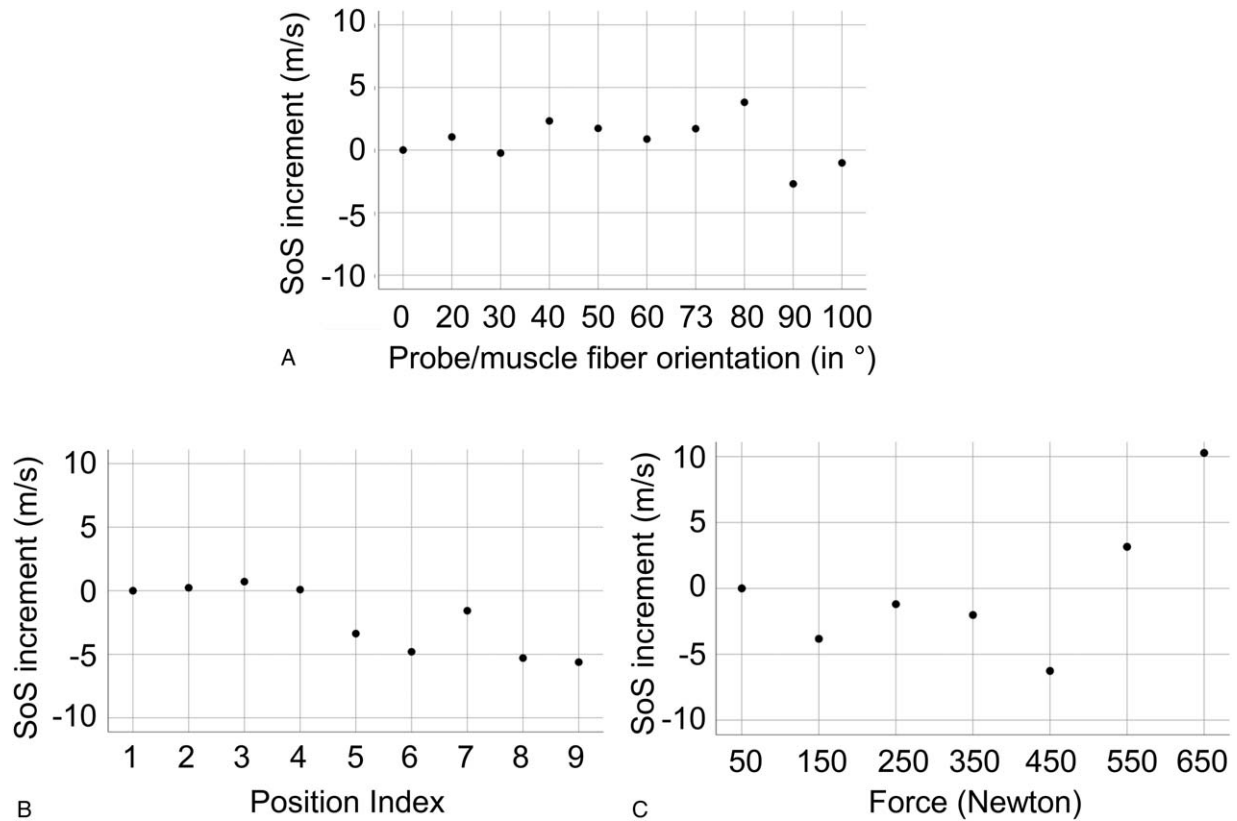
**Figure 7.** Confounders in Speed of Sound (SoS) measurements. Effects of varying probe/muscle fiber orientation (A), position (B) and muscle load (C) on Speed of Sound (SoS).

Ruby et al have shown a high repeatability (SD 3.21 m/s) and reproducibility for SoS measurements of the lower leg.[20] Similarly, in this study, SD values of less than 5 m/s were detected for varying probe-muscle fiber angles, positions within the muscle, muscle loading states, and repeated measurements. The variation range between the healthy and cast calves was larger than the variation range induced by confounders and repeated measurements.

For shear wave elastography, several authors have shown that muscle possesses anisotropic properties leading to significantly higher velocity values when the probe is oriented parallel to muscle fibers,[37–40] compared to orienting transverse to the fibers. In contrast to this, Topp et al and Marsh et al found only small differences for SoS with varying probe/muscle fiber direction,[41,42] which is in line with our results. Differences in shear wave elastography measurements with varying contraction/stretch states present a further limitation of musculoskeletal shear wave elastography.[16,17] In contrast, the effects of contraction states were small for SoS in our study, which is in-line with the results of Marsh et al.[41] Considering different positions within the muscle within a given range, we detected only small effects.

Magnetic resonance imaging and CT are currently the gold standard for muscle size and fat content assessment. Both methods have disadvantages since they require a medical institution. MRI is expensive and CT exposes the patient to ionizing radiation.

Ultrasound imaging is a perpetually evolving field with novel imaging parameters[19,43] and algorithms.[44–46] Several studies have investigated the potential of ultrasound for musculoskeletal diagnostics in recent years[47,48] and first clinical protocols have been established.[49–51] The Speed-of-Sound technique offers a quick, comfortable, cost-effective method, which correlates strongly with Dixon MRI, the reference standard for fat quantification.[20] It could be used as an additional tool in assessing severity of muscle loss and rehabilitation progress in post-trauma patients. Further fields of application include geriatrics (sarcopenia assessment) and neurology (post-stroke/spinal injury care).

Limitations of our study include limited coverage of the entire calf, the wide age range of the patients, lack of diversity in the type of injuries and the small sample size.

Giving an outlook, further steps include the investigation of a larger number of patients and of muscle composition of several muscle groups beyond the calf muscle, for instance, upper extremities and abdominal muscles.

## 7. Conclusion

There was a significant reduction in SoS in the cast calf compared to the non-cast calf, indicating a potential role of SoS as a biomarker in detecting immobilization-induced fatty muscular degeneration not visible on B-mode ultrasound.

## Acknowledgments

## Author contributions

## References

[1] Shaffer MA, Okereke E, Esterhai JLJr, et al. Effects of immobilization on plantar-flexion torque, fatigue resistance, and functional ability following an ankle fracture. Phys Ther 2000;80:769–80.

[2] Stevens JE, Walter GA, Okereke E, et al. Muscle adaptations with immobilization and rehabilitation after ankle fracture. Med Sci Sports Exerc 2004;36:1695–701.

[3] Yoshiko A, Yamauchi K, Kato T, et al. Effects of post-fracture non-weight-bearing immobilization on muscle atrophy, intramuscular and intermuscular adipose tissues in the thigh and calf. Skeletal Radiol 2018;47:1541–9.

[4] Deitrick JE. The effect of immobilization on metabolic and physiological functions of normal men. Bull N Y Acad Med 1948;24:364–75.

[5] White MJ, Davies CT, Brooksby P. The effects of short-term voluntary immobilization on the contractile properties of the human triceps surae. Q J Exp Physiol 1984;69:685–91.

[6] Haruna Y, Suzuki Y, Kawakubo K, et al. Decremental reset in basal metabolism during 20-days bed rest. Acta Physiol Scand Suppl 1994;616:43–9.

[7] Stuart CA, Shangraw RE, Prince MJ, et al. Bed-rest-induced insulin resistance occurs primarily in muscle. Metabolism 1988;37:802–6.

[8] Brooks N, Cloutier GJ, Cadena SM, et al. Resistance training and timed essential amino acids protect against the loss of muscle mass and strength during 28 days of bed rest and energy deficit. J Appl Physiol (1985) 2008;105:241–8.

[9] Sousa AS, Guerra RS, Fonseca I, et al. Sarcopenia and length of hospital stay. Eur J Clin Nutrition 2015;70:595.

[10] Lauritzen JB. Hip fractures: incidence, risk factors, energy absorption, and prevention. Bone 1996;18(1 Suppl):65S–75S.

[11] Wall BT, Dirks ML, van Loon LJ. Skeletal muscle atrophy during short-term disuse: implications for age-related sarcopenia. Ageing Res Rev 2013;12:898–906.

[12] Manini TM, Clark BC, Nalls MA, et al. Reduced physical activity increases intermuscular adipose tissue in healthy young adults. Am J Clin Nutr 2007;85:377–84.

[13] Jones SW, Hill RJ, Krasney PA, et al. Disuse atrophy and exercise rehabilitation in humans profoundly affects the expression of genes associated with the regulation of skeletal muscle mass. FASEB J 2004;18:1025–7.

[14] Sergi G, Trevisan C, Veronese N, et al. Imaging of sarcopenia. Eur J Radiol 2016;85:1519–24.

[15] Creze M, Nordez A, Soubeyrand M, et al. Shear wave sonoelastography of skeletal muscle: basic principles, biomechanical concepts, clinical applications, and future perspectives. Skeletal Radiol 2018;47:457–71.

[16] Gennisson JL, Deffieux T, Mace E, et al. Viscoelastic and anisotropic mechanical properties of in vivo muscle tissue assessed by supersonic shear imaging. Ultrasound Med Biol 2010;36:789–801.

[17] Aubry S, Nueffer JP, Carrie M. Evaluation of the Effect of an Anisotropic Medium on Shear Wave Velocities of Intra-Muscular Gelatinous Inclusions. Ultrasound Med Biol 2017;43:301–8.

[18] Szabo TL. Diagnostic Ultrasound Imaging: Inside Out. 1st Ed. Burlington: Elsevier Academic Press; 2004.

[19] Hambardzumyan and HayrapetyanDifferential diagnosis of malignant melanoma and benign cutaneous lesions by ultrasound analysis. Sci Med J 2020;2:2.

[20] Ruby L, Kunut A, Nakhostin DN, et al. Speed of sound ultrasound: comparison with proton density fat fraction assessed with Dixon MRI for fat content quantification of the lower extremity. Eur Radiol 2020;30:5272–80.

[21] Sconfienza LM. Sarcopenia: ultrasound today, smartphones tomorrow? Eur Radiol 2019;29:1–2.

[22] Pagano AF, Brioche T, Arc-Chagnaud C, et al. Short-term disuse promotes fatty acid infiltration into skeletal muscle. Cachexia Sarcopenia Muscle 2018;9:335–47.

[23] Gorgey AS, Dudley GA. Skeletal muscle atrophy and increased intramuscular fat after incomplete spinal cord injury. Spinal Cord 2007;45:304–9.

[24] Grimm A, Meyer H, Nickel MD, et al. Repeatability of Dixon magnetic resonance imaging and magnetic resonance spectroscopy for quantitative muscle fat assessments in the thigh. J Cachexia Sarcopenia Muscle 2018;9:1093–100.

[25] Ryan AS, Dobrovolny CL, Smith GV, et al. Hemiparetic muscle atrophy and increased intramuscular fat in stroke patients. Arch Phys Med Rehabil 2002;83:1703–7.

[26] Iversen E, Hassager C, Christiansen C. The effect of hemiplegia on bone mass and soft tissue body composition. Acta Neurol Scand 1989;79: 155–9.

[27] Ruby L, Sanabria SJ, Obrist AS, et al. Breast Density Assessment in Young Women with Ultrasound based on Speed of Sound: Influence of the Menstrual Cycle. Medicine (Baltimore) 2019;98:e16123. doi: 10.1097/MD.0000000000016123.

[28] Ramsay JW, Barrance PJ, Buchanan TS, et al. Paretic muscle atrophy and non-contractile tissue content in individual muscles of the post-stroke lower extremity. J Biomech 2011;44:2741–6.

[29] Frimel TN, Kapadia F, Gaidosh GS, et al. A model of muscle atrophy using cast immobilization in mice. Muscle Nerve 2005;32:672–4.

[30] Bach-Gansmo FL, Wittig NK, Bruel A, et al. Immobilization and long-term recovery results in large changes in bone structure and strength but no corresponding alterations of osteocyte lacunar properties. Bone 2016;91:139–47.

[31] Khalid M, Brannigan A, Burke T. Calf muscle wasting after tibial shaft fracture. Br J Sports Med 2006;40:552–3.

[32] Berg HE, Dudley GA, Haggmark T, et al. Effects of lower limb unloading on skeletal muscle mass and function in humans. J Appl Physiol 1991;70:1882–5.

[33] Hather BM, Adams GR, Tesch PA, et al. Skeletal muscle responses to lower limb suspension in humans. J Appl Physiol 1992;72:1493–8.

[34] Schulze K, Gallagher P, Trappe S. Resistance training preserves skeletal muscle function during unloading in humans. Med Sci Sports Exerc 2002;34:303–13.

[35] Gruther W, Benesch T, Zorn C, et al. Muscle wasting in intensive care patients: ultrasound observation of the M. quadriceps femoris muscle layer. J Rehabil Med 2008;40:185–9.

[36] Welch D, Ndanyo LS, Brown S, et al. Thigh muscle and subcutaneous tissue thickness measured using ultrasound imaging in older females living in extended care: a preliminary study. Aging Clin Exp Res 2018;30:463–9.

[37] Gennisson JL, Catheline S, Chaffai S, et al. Transient elastography in anisotropic medium: application to the measurement of slow and fast shear wave speeds in muscles. J Acoust Soc Am 2003;114:536–41.

[38] Cortez CD, Hermitte L, Ramain A, et al. Ultrasound shear wave velocity in skeletal muscle: a reproducibility study. Diagn Interv Imaging 2016;97:71–9.

[39] Eby SF, Song P, Chen S, et al. Validation of shear wave elastography in skeletal muscle. J Biomech 2013;46:2381–7.

[40] Gennisson JL, Grenier N, Combe C, et al. Supersonic shear wave elastography of in vivo pig kidney: influence of blood pressure, urinary pressure and tissue anisotropy. Ultrasound Med Biol 2012;38:1559–67.

[41] Marsh RL. Speed of sound in muscle for use in sonomicrometry. J Biomech 2016;49:4138–41.

[42] Topp KA, O'Brien WDJr. Anisotropy of ultrasonic propagation and scattering properties in fresh rat skeletal muscle in vitro. J Acoust Soc Am 2000;107:1027–33.

[43] Sanabria SJ, Martini K, Freystätter G, et al. Speed of sound ultrasound: a pilot study on a novel technique to identify sarcopenia in seniors. Eur Radiol 2019;29:3–12.

[44] Gao Z, Chung J, Abdelrazek M, et al. Privileged modality distillation for vessel border detection in intracoronary imaging. IEEE Trans Med Imaging 2020;39:1524–34.

[45] Gao Z, Wu S, Liu Z, et al. Learning the implicit strain reconstruction in ultrasound elastography using privileged information. Med Image Anal 2019;58:101534.

[46] Gao Z, Li Y, Sun Y, et al. Motion tracking of the carotid artery wall from ultrasound image sequences: a nonlinear state-space approach. IEEE Trans Med Imaging 2018;37:273–83.

[47] Chiu YH, Chang KV, Chen IJ, et al. Utility of sonoelastography for the evaluation of rotator cuff tendon and pertinent disorders: a systematic review and meta-analysis. Eur Radiol 2020;doi:10.1007/s00330-020-07059-2.

[48] Chang KV, Yang KC, Wu WT, et al. Association between metabolic syndrome and limb muscle quantity and quality in older adults: a pilot ultrasound study. Diabetes Metab Syndr Obes 2019;12:1821–30.

[49] Cruz-Jentoft AJ, Bahat G, Bauer J, et al. Sarcopenia: revised European consensus on definition and diagnosis. Age Ageing 2019;48:601.

[50] Ticinesi A, Meschi T, Maggio M, et al. Application of ultrasound for muscle assessment in sarcopenia: the challenge of implementing protocols for clinical practice. Eur Geriatr Med 2019;10:155–6.

[51] Imbault M, Faccinetto A, Osmanski BF, et al. Robust sound speed estimation for ultrasound-based hepatic steatosis assessment. Phys Med Biol 2017;62:3582–98.